Electronic (ESI) for Chemical Communications

Simultaneous reduction and surface functionalization of graphene oxide via an ionic liquid for electrochemical sensor

Chunfeng Wang, Yujuan Chen, Kelei Zhuo,* and Jianji Wang

School of Chemistry and Chemical Engineering, Key Laboratory of Green Chemical Media and Reactions, Ministry of Education, Henan Normal University, Xinxiang, Henan 453007, P. R.China

Materials and Methods

Materials

Graphite power (KS-10, 99.95%) was obtained from Sigma-Aldrich. 1-Methylimidazole (99%), *L*-cysteine (99%), *n*-Butyl bromide (99%), catechol (CT, AR, 99%), and hydroquinone (HQ, AR) were obtained from Aladdin Chem. Co. Ltd (Shanghai, China). Hydrazine hydrate (AR) was from Nanjing Chemistry Reagent Co. Ltd (Nanjing, China). Anion exchange resin (Ambersep 900 OH) was purchased from Alfa Aesar. All other chemicals were of analytical grade and used without further purification. All solutions were prepared with ultrapure water. Phosphate buffer solutions (PBS, 0.1 mol L^{-1}) were prepared by mixing the stock solution of 0.10 mol L^{-1} NaH_2PO_4 and 0.1 mol L^{-1} Na_2HPO_4, and the pH was adjusted by NaOH or HCl. The stock solution of 0.10 molL^{-1} CT or 0.10 mol L^{-1} HQ was freshly prepared by dissolving CT or HQ in boiling water and kept at 4°C. The stock solution was diluted to various concentrations by mixing with the buffer solution.

Characterization

The AFM measurements were performed on an Agilent 5500.

The UV-vis spectra measurements were obtained using a TU-1810 UV-vis Spectrophotometer.

The FTIR spectra measurements were measured on a Nicolet 6700 spectrophotometer.

The XRD measurements was performed on a Bruker D8 using Cu $K\alpha_1$ (1.54056 Å) radiation.

FESEM, EDX and EDS mapping measurements were obtained using a Hitachi S4800.

The Raman spectra measurements were taken on a Horiba Aramis.

The electrical impedance spectroscopy (EIS) and the electrochemical experiments measurements were measured on a CHI660D electrochemical workstation with a conventional three-electrode cell. A bare or modified GCE (CHI104, *d*=3 mm) was used as the working electrode. A saturated calomel electrode (SCE) and a platinum wire were used as the reference electrode and auxiliary electrode, respectively.

Preparation of the IL–G and the G

[Bmim][Cys] was prepared according to the procedure described in the literature.[1] A general procedure for the preparation of IL–G composites is described as follows. Typically, 0.5 g of the ionic liquid was

put into 10 mL GO aqueous suspension of 0.5 mg mL^{-1}. The mixture was kept in a tightly sealed glass bottle and stirred for 15 h at room temperature. Firstly, the black product was isolated by centrifugation at 8000 rpm, and then the obtained black slurry was washed with deionized water. Then, one part of the as-prepared products was dispersed in deionized water to prepare the suspension of IL–G, and the other part was used to produce the powder of IL–G by drying at 50°C for 24 h under vacuum. For comparison, the pristine graphene were also prepared by the reduction of hydrazine hydrate at 80°C for 24 h.

Because the reactions of GO with an excess of [Bmim][Cys] were performed, only little $[R–SH]^-$ anions of [Bmim][Cys] ionic liquids were oxidized into $[R–S–S–R]^{2-}$. Therefore, the ionic liquid in the IL–G composite should be mainly in its original chemical form, i.e. [Bmim][R–SH].

To help readers to understand the process of the chemical reaction, the chemical equation is shown as follows in Scheme S1.

Preparation of G and IL–G modified electrodes

Prior to modification, the glassy carbon electrode (GCE) was polished with 1.0, 0.3, and 0.05 μm alumina slurry to a mirror-like surface, then ultrasonically cleaned in water and dried in N_2 blowing. 5 μL of the IL–G suspension was dropped onto a polished GCE electrode and dried in ambient air for 2 h to obtain IL–G/GCE electrode. For comparison, G/GCE was also fabricated with the similar procedure. But the G was dissolved in dimethylformamide solution.

Stability, reproducibility and interference

In order to characterize the reproducibility of the IL–G/GCE, six IL–G/GCE electrodes were fabricated in parallel. The peak currents in the mixture containing 50 μmol L^{-1} CT and 50 μmolL^{-1} HQ was determined under the optimized conditions at the six modified electrodes. The relative standard deviation of the oxidation peak current was 2.1% for CT and 1.5% for HQ, respectively, indicating that the IL–G/GCE has good reproducibility. When the electrode was kept at 4℃ for ten days, the current responses retained more than 95% of the initial response, showing the excellent stability of the IL–G.

The influence of some possible interferences in wastewater was investigated by analyzing a standard solution of 50 μmol L^{-1} CT and 50 μmolL^{-1} HQ in pH = 7.0 PBS. It was determinated that 600 folds of K^+, Na^+, Ca^{2+}, Cu^{2+}, Al^{3+}, Fe^{3+}, Pb^{2+}, PO_4^{3-}, SO_4^{2-}, CO_3^{2-}, and Cl^- did not show interferences to the detection of CT and HQ. Moreover, 50-fold concentrations of ethanol and glucose did not show interference either.

Data analysis of thermogravimetric analysis

The samples were heated under the flow of N_2 to 800°C with a heating rate of 5°C min^{-1}. The mass loss of the IL (Fig. 1B, curve a) was nearly 100 wt% at 175–310°C. The mass loss of graphene (Fig. 1B, curve d) was approximately 3.6 wt% at 175–310°C, which could be assigned to the decomposition of residual oxygen-containing groups. The IL–G composites exhibited a much lower residue than graphene. The mass loss of the IL–G composites (Fig. 1B, curve c) at 175–310°C was approximately 16.5 wt% due to the decomposition of residual oxygen-containing groups and the IL. Therefore, the difference between the

mass loss of graphene and that of the IL–G composites should be the content of the attached IL to graphene, namely the IL content in the IL–G composites was approximately 12.9 wt%.

The linear regression equation of CT and HQ

The calibration curve for CT showed two linear segments: the first linear segment increased from 2 to 30 μmol L^{-1} with a linear regression equation: log I/μA = –1.378 – 0.103 log C/μmol L^{-1} (R = 0.9917), and the second linear segment increased up to 400 μmol L^{-1} with the linear regression equation: log I/μA = –0.926 – 0.411 log C/μmol L^{-1} (R = 0.9997). The calibration curve for HQ also showed two linear segments: the first linear segment increased from 1 to 30 μmol L^{-1} with a linear regression equation: log I/μA = –1.359 – 0.206 log C/μmol L^{-1} (R = 0.9978), and the second linear segment increased up to 300 μmolL^{-1} with linear regression equation: log I/μA = –1.152 – 0.346 log$C$/μmol L^{-1} (R = 0.9989).

Tables

Table S1. Performance comparison of the modified electrode for CT and HQ detection with other electrodes.

Electrode	Technique	Linear range (10^{-6} molL^{-1})		LOD (10^{-6} molL^{-1})		Reference
		CT	HQ	CT	HQ	
IL–CPE	DPV	–	10–1,500	–	4	(2)
G–chitosan/GCE	DPV	1–400	1–300	0.75	0.75	(3)
PDDA–G/GCE	DPV	1–400	1–500	0.20	0.25	(4)
G/GCE	DPV	–	1–10 and 10–80	–	0.8	(5)
MWNTs/GCE	DPV	0.6–100	1–100	0.2	0.75	(6)
CCM–CPE	AM	–	0.1–137.5	–	0.05	(7)
PASA/MWNTs/GCE	DPV	6–180	6–100	1	1	(8)
IL–G/GCE	DPV	2–30 and 30–400	1–30 and 30–300	1	0.85	This work

IL-CPE: ionic liquid modified carbon paste electrode; PDDA: poly(diallyldimethylammonium chloride); MWNTs: multi-wall carbon nanotubes; CCM-CPE: core-shell magnetic nanoparticles supported on carbon paste electrode; PASA: poly-amidosulfonic acid; DPV: differential pulse voltammetry, G: graphene, AM: amperometry.

Table S2. Determination of HQ and CT in water samples (n = 6).

Samples		Founded /(μmolL^{-1})	Added /(μmolL^{-1})	Total found /(μmolL^{-1})	RSD/%	Recovery/%
Tap water	CT	–	10.0	9.85	2.64	98.5
	HQ	–	10.0	10.26	3.51	102.6
River water	CT	–	100	103.4	3.88	103.4
	HQ	–	100	96.8	2.47	96.8

Simultaneous determinations of CT and HQ in local tap water and river water without any pretreatment were made for the assessment of possible applications of the modified electrode. Since the amounts of HQ and CT were unknown in water samples, the spike and recovery experiments were performed by measuring the DPV responses to the samples in which the known concentrations of HQ and CT were added. The amounts of HQ and CT in the water samples were then determined by calibration method and the results were showed in Table S2.

Scheme

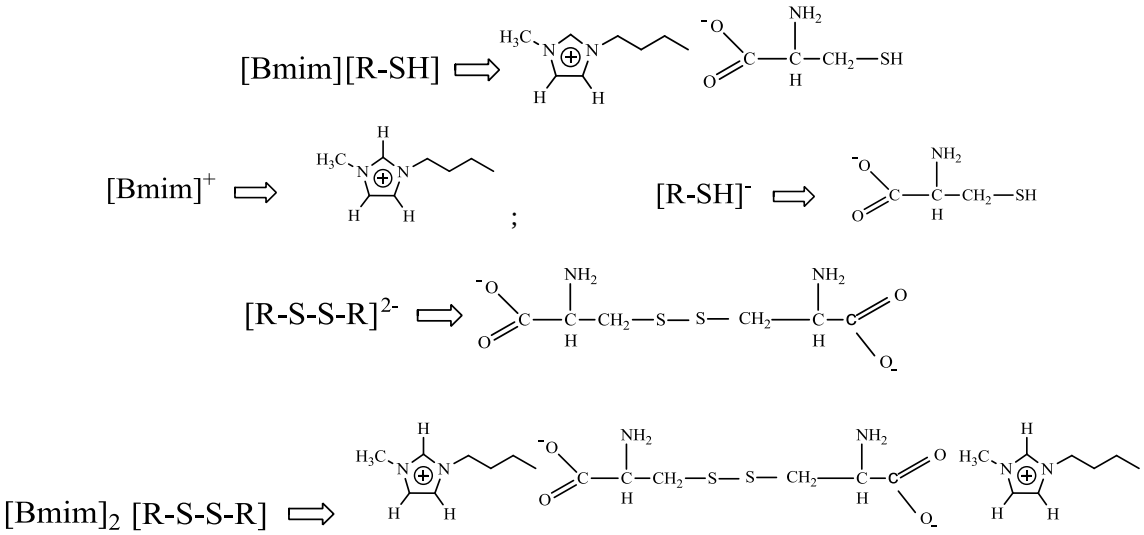

$$GO + [Bmim]\,[R\text{-}SH] \Rightarrow [Bmim]\,[R\text{-}SH]/Graphene + [Bmim]_2\,[R\text{-}S\text{-}S\text{-}R]$$

Scheme S1. A chemical equation of GO with [Bmim][R-SH] ([Bmim][Cys]). For the convenience in writing the chemical equation, some abbreviations were used and given in this scheme.

Figures

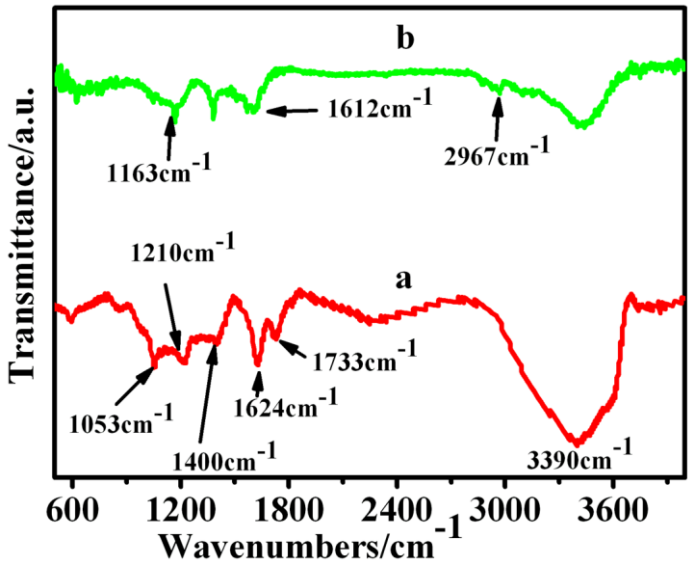

Fig. S1 FTIR spectra of GO (a) and the obtained IL-G composites (b).

For GO, the characteristic peaks for C=O stretching vibration appeared at 1733 cm^{-1}, and the characteristic peaks for O–H the stretching and deformation vibration appeared at 3390 cm^{-1} and 1400 cm^{-1}, respectively. Aromatic C=C stretching vibration showed at 1624 cm^{-1}, and the peaks at 1210 cm^{-1} and 1053 cm^{-1} could be attributed to the epoxy C–O stretching vibration and the alkoxy C–O stretching vibration, respectively. For the IL–G composites, the peak of the aromatic C=C group still existed and shifted to 1612 cm^{-1} after reduction by the IL. It suggested that the frame of sp^2 carbon atoms after reduction by the IL was retained well, as before.

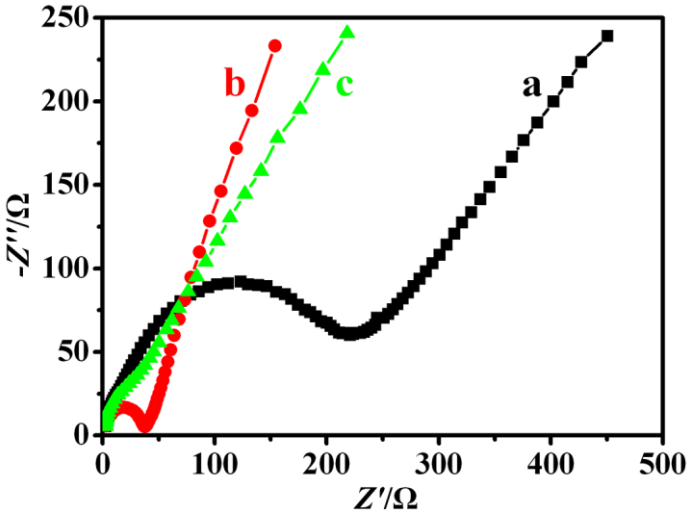

Fig. S2 Nyquist diagrams of electrochemical impedance spectra recorded from 1 to 10^5 Hz for $[Fe(CN)_6]^{3-}/[Fe(CN)_6]^{4-}$ (2.5 mmol L^{-1}, 1:1) in 0.5 molL^{-1} KCl: (a) bare GCE, (b) G/GCE, and (c) IL–G/GCE.

Fig. S2 illustrates the Nyquist plots of EIS for three different electrodes in the presence of redox probe, $Fe(CN)_6^{4-/3-}$. At the bare GCE (curve a) and the G/GCE (curve b), the redox process of the probes showed an electron-transfer resistance of about 225 Ω and 40 Ω, respectively, while the IL–G/GCE (curve c) displayed an almost straight line.

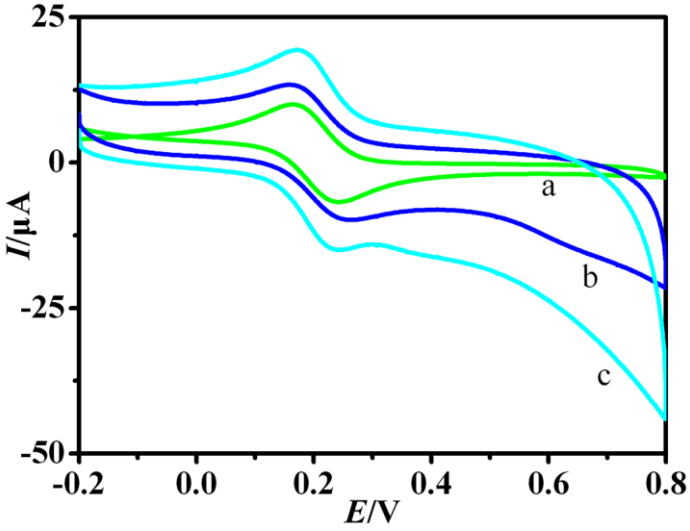

Fig. S3 Cyclic voltammograms at (a) bare GCE, (b) G/GCE, and (c) IL–G/GCE electrode in solution containing 5.0 mmol L^{-1} $Fe(CN)_6^{3-}$ and 0.1 mol L^{-1} KCl at a scan rate of 50 mV s^{-1}.

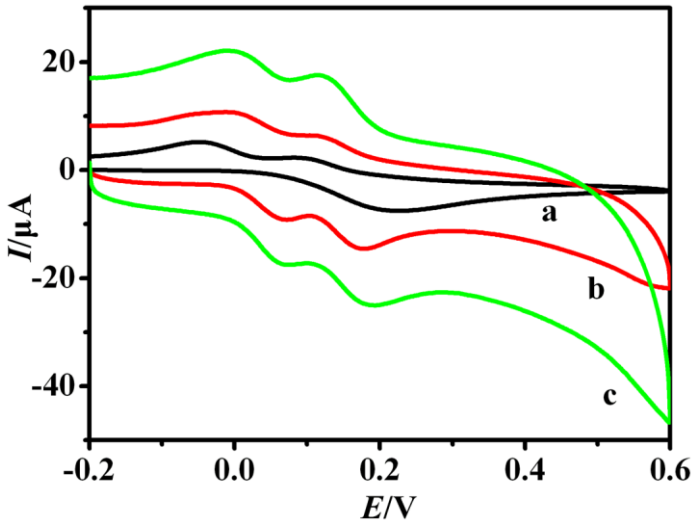

Fig. S4 CVs of 0.2 mmol L^{-1} CT and HQ in pH 7.0 PBS at different electrodes. (a) bare GCE, (b) G/GCE, and (c) IL–G/GCE. Scan rate: 50mV s^{-1}.

Fig. S4 shows the CVs of CT and HQ in pH = 7.0 PBS at the bare GCE, G/GCE, and IL–G/GCE, respectively. At the bare GCE (curve a), a broad oxidation peak and a pair of reduction peaks were observed, indicating that these peaks could not be separated at the bare GCE. However, at the G/GCE (curve b), two pairs of current peaks were observed clearly, showing that the oxidation and reduction peaks of CT and HQ could be separated. Compared to the G/GCE, the oxidation and reduction peak currents and peak separations increased further at IL–G/GCE.

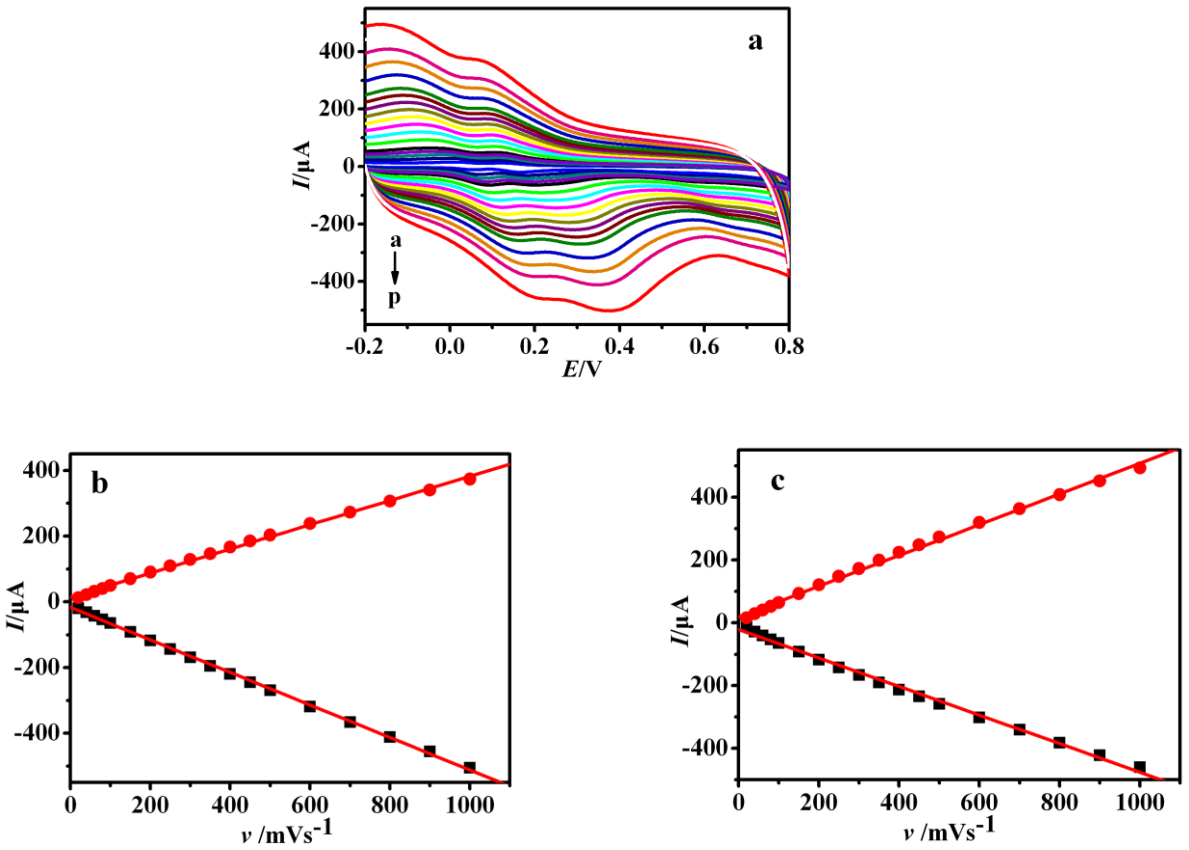

Fig. S5 a) Effect of scan rate on the redox behavior of 2×10^{-4} mol L^{-1} CT and HQ. (a–p) 20, 40, 60, 80, 100, 150, 200, 250, 300, 350, 400, 450, 500, 600, 700, 800, 900, and 1,000 mV s^{-1};b) The redox peak currents of CT *vs* scan rate; c) The redox peak currents of HQ *vs* scan rate.

Fig. S5 shows the influence of scan rate on electrochemical behavior of the two dihydroxybenzene isomers at the IL–G/GCE. As can be seen in Fig. S5a, the two redox peak currents for CT and HQ increased with increasing scan rate from 20 to 1000 mVs^{-1}. For CT (Fig. S5b), a pair of symmetrical redox peaks was obtained. The redox peak currents followed the linear regression equation of *I*pa/μA = –0.49*v*/mV s^{-1} – 16.64 (*R* = 0.9995) and *I*pc/μA = 0.37*v*/mV s^{-1} + 13.95 (*R* = 0.9990). For HQ (Fig. S5c), a pair of symmetrical redox peaks was also observed. The redox peak currents followed the linear regression equation of *I*pa/μA = –0.46*v*/mV s^{-1} – 20.87 (*R* = 0.9978) and *I*pc/μA = 0.49*v*/mV s^{-1} + 18.81 (*R* = 0.9985). These results indicated that the redox processes of CT and HQ were adsorption-controlled in the selected scan rate range.

Supporting References

1 K. Fukumoto, M. Yoshizawa and H. Ohno, *J. Am. Chem. Soc.*, 2005, **127**, 2398–2399.

2 Y. Zhang and J. B. Zheng, *Electrochim Acta*, 2007, **52**, 7210–7216.

3 H. S.Yin, Q. M. Zhang, Y. L. Zhou, Q. Ma, T. Liu, L.S. Zhu and S.Y. Ai, *Electrochim Acta*, 2011, **56**, 2748–2753.

4 L. T.Wang, Y. Zhang, Y. L. Du, D. B. Lu, Y. Z. Zhang and C. M. Wang, *J Solid State Electrochem*, 2012, **16**, 1323–1331.

5 S. J. Li and G. F. Wang, *Microchim Acta*, 2012, **176**, 163–168.

6 H. Qi and C. Zhang, *Electroanalysis*, 2005, **17**, 832-838.

7 Y. Zhang, G. M. Zeng, L. Tang, D. L. Huang, X. Y. Jiang and Y. N. Chen, *Biosens.Bioelectron.*, 2007, **22**, 2121–2126.

8 D. Zhao, X. Zhang, L. Feng, L. Jia and S. Wang, *Colloid. Surf. B*, 2009, **74**, 317–321.